

1 **How hot are the Cairngorms?**

2 Jon Busby^{1*}, Martin Gillespie² and Sev Kender¹

3

4 ¹ British Geological Survey, Keyworth, Nottingham, NG12 5GG, UK

5 ² British Geological Survey, West Mains Road, Edinburgh, EH9 3LA, UK

6 * Corresponding author (email: jpbu@bgs.ac.uk)

7

8

Synopsis

9 Heat flow measured over the East Grampians batholith in the 1980s was found to be
10 unexpectedly low and at odds with high radiogenic heat production within the outcropping
11 granites and a very large volume of granite predicted from an interpretation of gravity data.
12 Past climate variations perturb temperature gradients in the shallow sub-surface leading to
13 erroneous estimates of heat flow. A reconstruction of the surface temperature history during
14 the last glacial cycle has enabled a rigorous palaeoclimate correction to be applied to the heat
15 flow that shows an increase of 25% over previously reported values; revised to 86 ± 7 mWm⁻².
16 ². An interpretation of recent mapping reveals that the surface exposures of the East
17 Grampians granites are the roof zones of a highly evolved magma system. Rock composition
18 therefore is likely to become more mafic with depth and the heat production will decrease
19 with depth. This petrological model can be reconciled with the gravity data if the shape of the
20 batholith is tabular with deep seated feeder conduits. The increased heat flow value leads to
21 revised predictions of sub-surface temperatures of 129 °C at 5 km depth and 176 °C at 7 km
22 depth, increases of 40% and 49% respectively compared to previous estimates. These
23 temperatures are at the lower end of those currently required for power generation with
24 Engineered Geothermal Systems, but could potentially be exploited as a direct heat use
25 resource in the Cairngorm region by targeting permeable fractures with deep boreholes.

26

Introduction

27 Engineered Geothermal Systems (EGS) are reservoirs that have been created to extract
28 economical amounts of heat from low permeability and/or porosity geothermal resources
29 (MIT 2006). In regions of the world with average continental heat flows, EGS is often
30 associated with granites that have elevated concentrations of the naturally occurring
31 radioelements of uranium (U), thorium (Th) and potassium (K). Where large volumes of such
32 rocks occur, the radioactive decay of these elements produces heat anomalies at depth; these
33 intrusions are therefore known as high-heat producing (HHP) granites. The geothermal

34 energy they contain can in theory be exploited by pumping cold water down a borehole into a
35 zone of hot rocks where it is heated as it travels through fractures of an engineered reservoir
36 to a second borehole, from which it is extracted. The heat is then transferred to a binary fluid
37 (that has a lower boiling point than water) via a heat exchanger which then turns a turbine to
38 generate electricity. The highest reported heat flow in the UK of $\sim 130 \text{ mW m}^{-2}$ was measured
39 (Wheildon *et al.* 1981) in the Permian granite intrusions of Cornwall and Devon (surface
40 expressions of the Cornubian batholith) and these intrusions have been extensively
41 investigated as potential EGS reservoirs (e.g. Downing & Gray 1986a, b; Batchelor 1987;
42 Richards *et al.* 1994). The potential for EGS in Scotland was assessed during the Geothermal
43 Energy programme (Rollin 1982, 1984; Lee 1984; Webb & Brown 1984; Wheildon *et al.*
44 1984; Lee *et al.* 1984, 1987). There are no major late Carboniferous to Permian granite
45 intrusions in Scotland, and therefore no direct analogues of the south-west England
46 intrusions. The East Grampians batholith (EGB) underlies an east-west trending zone
47 extending inland from Aberdeen. Many large Siluro-Devonian granite intrusions crop out
48 within this zone and, from geochemical determinations of U, Th and K a number were found
49 to have the highest heat production (HP) values in the UK (Webb & Brown, 1984) (see Table
50 1 and Figure 1). Subsequent heat flow measurements in shallow boreholes ($\sim 300 \text{ m}$ deep) at
51 Cairngorm, Mount Battock, Ballater and Bennachie of 70, 59, 71 and 76 mWm^{-2} respectively
52 were much lower than anticipated from the heat production data (Wheildon *et al.* 1984) and
53 were therefore disappointing.

54 The East Grampians batholith is associated with an extensive Bouguer gravity anomaly low
55 that has a minimum magnitude of -53 mGal (see Figure 2). Modelling of this gravity anomaly
56 (Rollin 1984, 2009) suggested that the granite intrusions may extend to between 9 and 13 km
57 depth as one large intrusive mass with an approximate volume of granite of 25000 km^3 . In
58 order to reconcile the disparity between high heat production and low heat flow, Wheildon *et*
59 *al.* (1984) modelled the heat flow at each of the heat flow boreholes. It was concluded that
60 heat production must decline rapidly with depth within the granite and that the background
61 regional heat flow must be relatively low. The rapid decrease in heat production was ascribed
62 to strong vertical fractionation of the radiothermal elements; in other words, the
63 concentrations of U, Th and K diminish rapidly with depth, so that the HHP character of the
64 intrusions is just a near-surface feature. This interpretation was based, to a large extent, on a
65 theoretical understanding of granite magma evolution, the geochemical data derived from
66 samples from the relatively narrow vertical range spanned by the boreholes ($\sim 300 \text{ m}$) and

67 surface exposures (Webb & Brown 1984; Webb *et al.* 1985). The heat flow modelling
68 therefore predicted a sub-surface temperature at 5 km depth of 92°C. When considered
69 against predicted temperatures of 182°C at 5 km depth for parts of the Cornubian Batholith
70 (Downing & Gray 1986a) the East Grampians were judged as geothermally unprospective.

71 It is known that past climate change can perturb sub-surface temperature gradients from
72 which heat flow is calculated (e.g. Benfield 1939; Birch 1948; Crain 1968; Jessop 1971; Beck
73 1977). In Britain, warming since the last glaciation would result in a positive correction to
74 heat flow which Younger *et al.* (2012) and Westaway & Younger (2013) suggested to be of
75 the order of $\sim 20 \text{ mW m}^{-2}$. Corrections to heat flow for palaeoclimate were not originally
76 applied to the East Grampians heat flow boreholes (Downing & Gray 1986a). The reason
77 stated was that it was unnecessary for comparative regional studies, although this would then
78 preclude using heat flow for predicting temperatures at depth. Westaway & Younger (2013)
79 have recently published a climate corrected heat flow value for the Ballater borehole of 89.5
80 mWm^{-2} , a 26% increase over the original value. Hence, it is quite likely that a lack of
81 consideration of palaeoclimate has resulted in an underestimate of heat flow, and by
82 implication geothermal potential, of the East Grampians.

83 This paper presents a rigorous palaeoclimate correction to East Grampians heat flow and,
84 with more recent petrological data on the intrusions, considers the implications for the
85 geothermal resource.

86 **The East Grampians heat flow boreholes**

87 As part of the UK Geothermal Energy Programme (Downing & Gray 1986a) heat flow
88 boreholes were drilled into the Cairngorm, Mount Battock, Ballater and Bennachie intrusions.
89 The Monadhliath intrusion, which is also of HHP character, was not included due to poor
90 accessibility. In each case a single vertical borehole was sunk to around 300 metres and core
91 was recovered in three short (<7 metre) sections at approximately 100, 200 and 300 metres
92 (amounting to $\sim 5\%$ of the total drilled depth). HP values for surface samples were affected by
93 uranium mobility in the surface and near-surface environment, so a second set of ‘preferred’
94 HP values were calculated from unweathered rock recovered in core discs and chippings. The
95 four intrusions consist of granite *sensu stricto* with subordinate proportions of coarser
96 (pegmatitic) and finer (microgranitic and aplitic) granitic rock. Variations in grain-size and in
97 the degree to which phenocrysts of feldspar are developed are characteristic features of all the
98 intrusions, and this textural heterogeneity is the main basis for recognising and mapping

99 internal divisions. Zones of hydrothermally altered rock, which probably formed shortly after
100 emplacement, are common. The passage of hot water through these zones has produced a
101 range of secondary minerals (notably hematite, epidote and chlorite), quartz veining and
102 joints, which act to locally weaken the rock mechanically, lower its overall thermal
103 conductivity and raise its permeability.

104 Downhole temperatures were measured with a thermistor probe suspended on a cable that
105 was calibrated against a platinum resistance thermometer and was capable of measuring in-
106 hole temperatures to $\pm 0.01^\circ\text{C}$. Due to the transient disturbance of downhole temperatures by
107 the drilling, borehole temperatures were monitored for several months until no change was
108 observed before an equilibrium temperature log was run. Thermal conductivities of recovered
109 borehole samples were measured with the divided bar technique using discs cut from the
110 cored sections and chippings for the rest of the boreholes. Samples were flooded with water
111 under vacuum and subjected to axial stress up to 7 MPa in the divided bar in order to simulate
112 natural conditions (Wheildon *et al.* 1984).

113 **Calculation of heat flow**

114 There are a number of techniques for calculating heat flow. The heat flow Q_d at depth d is
115 given by

$$Q_d = \lambda_d \times \left(\frac{\delta T}{\delta z} \right)_d \quad (1)$$

116 where $(\delta T/\delta z)_d$ is the temperature gradient over the interval of thermal conductivity λ_d . A
117 technique that combines all the observations from the borehole is the step-integrated heat
118 flow equation of Bullard (1939). The relationship between the thermal resistance R and the
119 temperature T is linear for conductive, steady-state vertical heat flow with no internal heat
120 production, i.e.

$$T_z = T_o + Q \sum_i \left(\frac{\Delta z_i}{\lambda_i} \right) \quad (2)$$

121 Where $R = \sum_i \left(\frac{\Delta z_i}{\lambda_i} \right)$, λ_i is the thermal conductivity of the i th layer of thickness Δz_i , T_o is the
122 mean ground surface temperature and Q is the heat flow. Wheildon *et al.* (1984) used
123 equation (2) when calculating the original heat flow values for the East Grampians intrusions.
124 Errors can be introduced when using the step integrated heat flow equation if any sections of
125 the borehole are subjected to convective heat transport; an indication of this is shown by

126 irregular temperature gradients. Hence, for this study, heat flow in each borehole has been re-
127 calculated using equation (1) over several 20-30 m thick intervals, at or below 100 m, that are
128 associated with uniform temperature gradients. The quoted, uncorrected, heat flow for each
129 borehole is the average of the interval measurements and these new values are shown in
130 Table 1. Two heat flow values are shown for Bennachie. This is because there is an increase
131 in measured thermal conductivity in the depth interval 210-280 m that is not associated with a
132 decrease in the temperature gradient. This implies that there may be an error in the thermal
133 conductivities from the lower section of the borehole, although Wheildon *et al.* (1984) did not
134 discuss these higher thermal conductivities. Hence for Bennachie one heat flow measurement
135 is based on an analysis of the whole borehole (90-280 m), whilst a second is calculated from
136 measurements in the upper section (90-200 m) of the borehole.

137

Correction for palaeoclimate

138 It is necessary to apply a correction for the effects of past climate variations as these will
139 perturb temperature gradients in the ground from which heat flow is calculated. For
140 simplified modelling purposes palaeoclimate can be considered as a series of one-off surface
141 temperature changes that will affect sub-surface temperatures depending on the magnitude of
142 the change in surface temperature and the time that has elapsed since the change. A surface
143 temperature history for the Quaternary consists of a series of cyclical (e.g. glacial–interglacial
144 cycles) to pseudo-cyclical (e.g. Dansgaard-Oeschger events) changes in temperature between
145 warmer and colder conditions. Each cycle can last from a few hundred to several thousand
146 years. The change in surface temperature will propagate into the ground, but the amplitude of
147 the change will decrease exponentially with depth and there is a time lag between the
148 temperature perturbation at the surface and at depth. The rate of the exponential decrease and
149 the time lag are both dependent on the thermal diffusivity of the geological strata.
150 Representing the surface temperature history as a series of step changes in temperature,
151 Carslaw & Jaeger (1959) have shown that

$$T_{\theta} = T_0 \times \operatorname{erfc} \left[z / 2\sqrt{\kappa t} \right] \quad (3)$$

152

153 where T_{θ} is the departure from original equilibrium temperature at depth z and time t after an
154 instantaneous change in surface temperature of T_0 ; κ is the average thermal diffusivity of the
155 geological strata down to depth z and $\operatorname{erfc}(x)$ is the complementary error function. Noting that
156 the change in surface temperature is the difference in temperature between successive steps,
157 the effect of more than one temperature step is found by addition of all the steps, i.e.

158
$$T_{\theta} = \sum T_{\theta i} \quad (4)$$

159 Where $T_{\theta i}$ is the temperature deviation due to the i th event (Beck 1977; Beardsmore & Cull
160 2001). An account of the theory for palaeoclimate correction from first principles is given by
161 Westaway & Younger (2013). This temperature deviation is subtracted from the measured
162 temperature to generate the undisturbed temperature distribution in the ground from which a
163 palaeoclimate corrected heat flow is calculated.

164

Surface temperature history

165 For the East Grampians region the magnitude of the climate correction to heat flow depends
166 on the surface thermal history during the last glacial-interglacial cycle, considered to extend
167 back to 126 kyr BP (thousand years before present) and in particular the extent of warming
168 since the coldest period (often referred to as the Last Glacial Maximum or LGM, ~20 kyr
169 BP). There are several proxies for past land surface temperature, which include fossil pollen
170 and beetle assemblages, and although each has its uncertainties, multiple proxy data used
171 together can provide reasonably robust reconstructions. Some generalised surface
172 temperature histories have been published; Beck (1977) generated a thermal history for the
173 northern hemisphere at three different latitudes and Westaway & Younger (2013) attempted a
174 reconstruction for the southern and northern UK over the last 150 kyr based on a combination
175 of climate proxy records including sea surface temperature (SST) and ice core temperature
176 data. The approach here has been to produce a surface temperature history specific to the
177 Cairngorms region, rather than to use a regionalised temperature history (c.f. Westaway &
178 Younger 2013). We attempt to capture the localised advance and retreat of glacier ice and the
179 temperature beneath the ice, which can vary rapidly over relatively short distances (Hall &
180 Glasser 2003). This has been achieved by reconstructing the shape of the last glacial-
181 interglacial cycle temperature history for the UK from nearby mean annual air temperature
182 (MAAT) reconstructions, scaling the curve for the Cairngorms latitude and modifying the
183 surface temperature for periods of ice cover. This is detailed below.

184 *Time interval 0–12 kyr BP*

185 For this interval pollen records are available across Europe, including the UK, which have
186 been quantitatively analysed by Davis *et al.* (2003). Based on this large dataset (500 sites),
187 these authors produced MAAT records for six different regions of Europe. The ‘central west’
188 MAAT curve has been followed for the last 12 kyr (Figure 3), as this is the region in closest
189 proximity to the UK. In this reconstruction the temperature anomaly (relative to present day
190 temperature) for the Younger Dryas (11-12 kyr BP) is -4°C .

191 *Time interval 12–22 kyr BP*

192 This important interval encompasses the LGM and the complicated, subsequent, deglaciation
193 (transition from the LGM to the onset of the current, Holocene, interglacial). The most
194 comprehensive analysis of the MAAT history for this interval is provided by the study of
195 Shakun *et al.* (2012) which summarises 80 records of both sea surface and land surface
196 proxies to reconstruct global latitudinal temperature curves. Their temperature curve
197 corresponding to 30–60°N is used here (Figure 3).

198 *Time interval 22–40 kyr BP*

199 For this interval there are no available regional time-series compilations of MAAT, and
200 therefore proximal NE Atlantic SST records have been used to estimate the shape of the UK
201 MAAT curve. For 22–40 kyr the proximal SST record from ocean core BOFS
202 (Biogeochemical Ocean Flux Study) 5K (Figure 3) was referenced; this site is located west of
203 the Porcupine Seabight at a similar latitude to the southern UK (Maslin *et al.* 1995). This is
204 believed to be a reasonably accurate estimate due to the proximity of the site, and similarity
205 to the Davis *et al.* (2003) and Shakun *et al.* (2012) compilation curves from the 0–22 kyr
206 interval (Figure 3). For BOFS 5K, both summer and winter absolute temperatures are
207 reconstructed by using planktonic foraminiferal assemblage data and different transfer
208 functions which all show similar trends (Figure 3).

209 *Time interval 40–140 kyr BP*

210 Finally, for the longer oldest time interval, the NE Atlantic SST reconstruction from ocean
211 core ODP 980 has been used (Figure 3), which is located in the Rockall Trough at a similar
212 latitude to the central UK (McManus *et al.* 1999). This record has some similarities to BOFS
213 5K, but is at a far lower temporal resolution and is therefore only applied to the older interval.

214 *Scaling the MAAT curve*

215 In order to scale the idealised MAAT curve (Figure 4 middle panel) modern MAAT is
216 applied as the Holocene average (maximum temperature), and the Annan and Hargreaves
217 (2013) global estimate of MAAT during the LGM (19–23 kyr BP) is used as a guide for the
218 minimum temperature, with a linear scaling of temperature between. The Annan &
219 Hargreaves (2013) dataset is based on a combination of computer modelling and pollen
220 MAAT proxies, where northern England and Scotland localities are 12–20°C below present.
221 Therefore, the minimum MAAT for the Cairngorms during the LGM has been estimated as
222 17°C below modern (present day) temperatures. This estimated temperature anomaly
223 of -17°C below present day temperatures for the Cairngorm region can be compared against

224 regional estimates. The average global estimate for the LGM fits reasonably well with the NE
225 Atlantic SST records, which show $\sim 11^{\circ}\text{C}$ offset between Holocene and LGM values at BOFS
226 5K (Maslin *et al.* 1995), and $\sim 8^{\circ}\text{C}$ offset at ODP 980 (McManus *et al.* 1999). The anomaly is
227 slightly greater than the SST estimates of the oceans surrounding the UK published by
228 MARGO *et al.* (2009), which were based on a synthesis of global integrated fossil and
229 geochemical proxies. It also fits well with pollen based reconstructions at 21 kyr BP from
230 central Europe (Bartlein *et al.* 2011) and NE France (Busschers *et al.* 2007), showing MAAT
231 $\sim 10^{\circ}\text{C}$ below present, and the pollen-based European regional reconstructions for the
232 Younger Dryas (12-11 kyr) at $\sim 4^{\circ}\text{C}$ below present (Davis *et al.* 2003).

233 *Effect of ice cover*

234 Due to the insulating capacity of ice sheets, the final land surface temperature estimates will
235 differ from the estimated MAAT during periods of glacier ice cover. Hence, it is necessary to
236 reconstruct the times at which the East Grampians were covered by glacier ice. This has been
237 modelled by several studies (e.g. Siegert & Dowdeswell 2004; Hubbard *et al.* 2009; Evans *et*
238 *al.* 2009; Clark *et al.* 2012). The British Ice Sheet reconstructions of Hubbard *et al.* (2009)
239 provide a series of time-slices with reconstructed ice sheet extent since 35 kyr BP. To
240 reconstruct the presence of an ice sheet in the older part of the record two scenarios have
241 been modelled. A number of authors have presented evidence for glaciations during this older
242 period (e.g. Clapperton 1997; Stoker & Bradwell 2005; Stewart & Lonergan 2011), so in the
243 first scenario glacier ice is assumed in the period 35–120 kyr BP whenever the reconstructed
244 temperature is at or below that during the period 12–35 kyr BP where Hubbard *et al.* (2009)
245 modelled the presence of glacier ice in the East Grampians region. Thus, ice cover is assumed
246 continuously from 110 kyr to 12 kyr BP. However, some authors dispute the presence of
247 older ice cover (e.g. Westaway & Younger, 2013) and so in the second scenario it is assumed
248 the Cairngorm region is only covered by glacier ice during the period 37 to 12 kyr BP.

249 Temperatures at the base of the Scottish ice sheet were discussed by Glasser & Siegert (2002)
250 and Hall & Glasser (2003). Wet-based ice that is often found under thick ice in topographical
251 troughs is warmer than dry-based ice frozen to its bed. Temperatures at the base of the ice
252 will also be affected by the mean annual air temperature. Sliding at the base of ice sheets may
253 be due to the pressure being close to the pressure melting point; a sufficiently high pressure
254 that the ice melts even though its temperature is below 0°C . Hall & Glasser (2003) have
255 shown that during basal freezing conditions, basal temperatures can range from -12°C to -6°C
256 (absolute). However, when basal melting occurs, basal temperatures are more likely to be in

257 the range of -1°C to $+1^{\circ}\text{C}$ (absolute). The results of Hall & Glasser (2003) have been used to
258 assign basal ice temperatures for the four heat flow borehole localities considered here. For
259 the period 110-37 kyr BP a pre-glacial topography is assumed, whilst present-day topography
260 is used for the period 37-12 kyr BP. The Mount Battock, Bennachie and Ballater boreholes
261 are all in valleys, hence a basal ice temperature of 0°C is assumed for the period 110-37 kyr
262 BP and $+1^{\circ}\text{C}$ (absolute) for 37-12 kyr BP. The Cairngorm borehole is situated at a higher
263 elevation (616 m compared to ~ 220 m for the other boreholes) and is on the upper slope of a
264 valley. Assumed basal ice temperatures are therefore -3°C (absolute) for the period 110-37
265 kyr BP and -2°C (absolute) for 37-12 kyr BP. These surface temperature histories are shown
266 in Figure 5.

267 Heat flow from each of the boreholes has been corrected for the surface temperature histories.
268 There are two alternative corrections reflecting the two scenarios of continuous ice cover
269 from 110-12 kyr BP (scenario 1) and ice cover only for the period 37-12 kyr BP (scenario 2).
270 These corrections are listed in Table 1 and demonstrate that the palaeoclimate correction is
271 large, approximately 24-28% of the raw (uncorrected) heat flow.

272 **Corrections for topography**

273 Heat flow is also affected by topography as heat will preferentially diffuse into valleys
274 resulting in an over estimate of heat flow in valleys, but an underestimate on hills and
275 mountains. As the heat flow boreholes in the East Grampians region were all in valley
276 locations heat flow will have been over estimated. Wheildon *et al.* (1984) applied a
277 topographic correction using an analytical three-dimensional treatment of topography,
278 described by Bullard (1940), and the heat flow values quoted in the Introduction above
279 include this correction. Westaway & Younger (2013) also discussed topographic corrections
280 and adapted a method by Lees (1910) for mountain ranges so that it could be applied to
281 valley locations. In this method a 2D topographic profile perpendicular to the valley axis is
282 fitted according to a mathematical form, referred to as a Lees Valley. From the fit, a series of
283 parameters are obtained from which the temperature perturbation arising from the valley is
284 easily calculated at any depth and location along the profile. From knowledge of thermal
285 conductivity this can be converted to a perturbation to heat flow via equation (1). For the
286 depth range 100-290 m Westaway & Younger (2013) calculated a topographic heat flow
287 correction of -5.7 mWm^{-2} for the Ballater borehole. The Lees Valley method has been applied
288 here to Ballater for each of the intervals over which heat flow was calculated and the average
289 for the depth range 140-280 m is -5.8 mWm^{-2} . The value quoted by Wheildon *et al.* (1984)

290 for Ballater is -4.2 mWm^{-2} , which is in close agreement with those derived using the Lees
291 Valley method. Therefore heat flow topographic corrections for the Cairngorm, Mount
292 Battock and Bennachie boreholes have not been repeated using the Lees Valley method and
293 the corrections of Wheildon *et al.* (1984) are used. These are shown in Table 1 along with a
294 final corrected heat flow for each borehole.

295 **New insights into the geology and petrogenesis of the East Grampians Batholith**

296 All of the East Grampians intrusions have been re-mapped since the mid-1980s (British
297 Geological Survey 1989; 1992; 1993a,b; 1995a,b,c; 1996a,b; Harrison 1987; Thomas *et al.*
298 2004). The new maps and descriptions reveal aspects of their character and emplacement
299 history in considerably more detail than was known previously. A feature of all the intrusions
300 (and of the nearby Monadhliath intrusion, which is similar lithologically and also has HHP
301 character), is the sense of a complicated emplacement history. The two larger intrusions
302 (Cairngorm and Mount Battock) in particular display patterns indicating multi-phase
303 emplacement of magma batches that over time became smaller and increasingly scattered
304 within the confines of the intrusion. Two-phase texture, caused when magma is emplaced
305 forcefully into a nearly-solidified rock causing it to brecciate, is another relatively common
306 feature of the East Grampians intrusions, providing further support for a complicated, multi-
307 phase emplacement history. This character may in part reflect the compositional similarity of
308 the various batches of magma, which probably lacked the contrasts in density and viscosity
309 that are believed to yield more ordered arrangements, such as concentric zoning, in some
310 intrusions. However, the large number of discrete mappable units and their lack of spatial
311 order contrast markedly with other well-characterised granite intrusions of broadly the same
312 age in Scotland, which display simple, concentrically zoned patterns at outcrop; these include
313 the Ben Rinnes, Lochnagar, and Peterhead plutons (Stephenson & Gould 1995), the Fleet
314 pluton (Stephens 1999) and the Ross of Mull pluton (Highton 1999).

315 It seems likely that HHP character, highly evolved magma compositions, disordered
316 emplacement patterns, and fluid enrichment are related features in the four studied East
317 Grampians intrusions. The presently exposed surface through each one probably lies near to
318 (<2 km below) the former intrusion roof (Thomas *et al.* 2004), in a zone situated at the top of
319 the evolving magma system. Within this zone, multiple batches of highly fractionated,
320 radiothermal granite magma were emplaced in rapid succession. Much of the magma
321 fractionation may have occurred prior to emplacement, at deeper levels in the system, and
322 there was probably little additional fractionation following emplacement. The radiothermal

323 elements therefore may not be vertically fractionated within the zone exposed at outcrop.
324 This zone is likely to be of limited vertical extent - perhaps 1-2 km - and a vertical diminution
325 in the concentration of radiothermal elements may only become apparent over a depth range
326 of this size. Fluid exsolving from the magma (and perhaps also entering the system from
327 adjacent country rocks) initially caused pervasive alteration of crystallised minerals (mainly
328 feldspars), but became increasingly partitioned into discrete zones as the magma solidified.

329 The Hill of Fare, Lochnagar, Glen Gairn and Peterhead intrusions crop out in the same E-W
330 trending zone as the four intrusions studied in the Geothermal Energy programme, and a
331 shared set of geochemical and petrological attributes (and similar age) led Stephens &
332 Halliday (1984) to propose that they all share a genetic relationship and therefore constitute a
333 suite - the 'Cairngorm Suite'. Stephens & Halliday (1984) did not include intrusions north of
334 the Great Glen Fault in their study, but the Helmsdale intrusion and possibly one or two
335 others in this region appear to share the same set of attributes and may be related genetically
336 to the East Grampians intrusions. These other intrusions of the Cairngorm Suite have HP
337 values in the range 2.2-4.1 μWm^{-3} (Brown *et al.* 1982) and therefore lack the very high HP
338 values of the four studied intrusions. They also lack evidence for fluid enrichment, and they
339 have more organised emplacement patterns - the Lochnagar, Peterhead and Ben Rinnes
340 intrusions are concentrically zoned at outcrop (Stephenson & Gould 1995). These intrusions
341 may therefore give an indication of what the Cairngorm, Mt Battock, Ballater and Bennachie
342 intrusions are like at levels a few kilometres below their present outcrop.

343 Webb & Brown (1984) showed that HP values calculated from surface samples were around
344 20-30% lower than those in equivalent rocks collected from borehole cores, because uranium
345 is easily leached in near-surface bedrock. The range of HP values for these other intrusions of
346 the Cairngorm Suite rises to 2.6-4.9 μWm^{-3} after a correction of 20% is applied to allow for
347 inferred uranium leaching. The East Grampians granite intrusions have such highly evolved
348 compositions that the nature of their source rocks has not been deduced with certainty. They
349 display I-type characteristics (formed mainly from melted igneous rock), but were considered
350 by Stephens & Halliday (1984) to be transitional between I-type and A-type (formed from
351 melted high-grade metamorphic rocks). If they are I-type, the intrusions may be vertically
352 stratified, with granite at outcrop and progressively less evolved compositions (e.g.
353 granodiorite, diorite and cumulate mafic rocks) at deeper levels.

354

Discussion

355 The palaeoclimate corrections clearly indicate that a substantial underestimation of heat flow
356 has occurred by not considering the effect of past climate. The two scenarios of continuous
357 ice cover from 110-12 kyr BP (scenario 1) and ice cover only for the period 37-12 kyr BP
358 (scenario 2) have produced a very similar result. This is because at the shallow depths of the
359 East Grampian boreholes, the main palaeoclimate influence is the warming that has taken
360 place since the LGM during the last 18 kyr. The difference in the two climate scenarios
361 occurs for the period prior to 37 kyr, which would have a greater influence on the
362 palaeoclimate correction for heat flows calculated from greater depths. The palaeoclimate
363 correction for each borehole has been taken as the mean of the two climate scenarios and
364 these range from 20.7 to 17.9 mWm⁻². The Bennachie borehole yields the highest value, but
365 also has the largest error due to the discrepancy in thermal conductivities between the upper
366 and lower sections of the borehole. For the analysis at Bennachie three heat flow
367 determinations were made in the interval 90-200 m and three in the interval 200-280 m.
368 Hence, the upper part of the borehole generates a lower value of corrected heat flow ($89.9 \pm$
369 2.1 mW m^{-2}) compared to the lower part ($111.9 \pm 1.4 \text{ mW m}^{-2}$). There is no discussion in
370 Wheildon *et al.* (1984) as to the change in thermal conductivity, but the high values in the
371 lower part of the borehole appear suspect. In Table 1 heat flows are listed for the average of
372 the whole borehole and the average for the upper section. Overall, the measured heat flow
373 from the four boreholes of the East Grampians shows a substantial increase over that
374 previously reported as a result of correction for palaeoclimate. The percentage increases are
375 27%, 29%, 24% and 18% for the Cairngorm, Mount Battock, Ballater and Bennachie (upper
376 section) boreholes respectively. Combining these borehole heat flows gives a mean revised
377 heat flow for the East Grampians batholith of $86 \pm 7 \text{ mWm}^{-2}$, an increase of 25% over the
378 previously reported values of Wheildon *et al.* (1984).

379 The gravity modelling of Rollin (1984; 2009) represented the granites as large volumes with
380 steeply outward-dipping straight (or slightly convex) sides extending to considerable depth
381 (9-13 km) with either a flat or curved base, modelled with a mean granite density of 2.62 Mg
382 m⁻³. This can be considered as the traditional view of how granites are intruded into the upper
383 crust. This gravity modelling is at odds with the revised petrological evidence where it is
384 expected that the East Grampians intrusions become increasingly mafic, and therefore denser,
385 with depth. More recent published work (e.g. Cruden 1998; Petford *et al.* 2000; Taylor 2007)
386 indicates that granites more commonly have a tabular form reflecting upward travel of
387 magma through one or several near-vertical, narrow (1 – 50 m wide) conduits. Spreading-out

388 of the magma at higher crustal levels results in thinner granite (a few kms thick) with
 389 potentially very thick granite over the feeder conduits. The Bouguer gravity anomaly at the
 390 Cairngorm and Ballater borehole sites is -46 mGal and is -28 and -38 mGal at the Bennachie
 391 and Mount Battock borehole sites respectively. Assuming a tabular space form for the East
 392 Grampians batholith this may indicate a central, west-east orientated conduit (beneath
 393 Cairngorm and Ballater) and thinner tabular lobes to the north and south (beneath Bennachie
 394 and Mount Battock). The revised heat flow value for Mount Battock is the lowest, possibly
 395 reflecting thinner granite, although the heat flow values for Cairngorm, Ballater and
 396 Bennachie are virtually the same.

397 Sub-surface temperature profiles, based on the revised heat flow determinations, and taking
 398 into consideration the nature of the East Grampians batholith, have been made. It is assumed
 399 that the Cairngorm, Mount Battock, Ballater and Bennachie intrusions are part of the roof
 400 zone of the evolved magma system and, due to vertical fractionation, the concentration of
 401 radiothermal elements diminishes with depth. Other intrusions of the Cairngorm suite may
 402 give an indication of reduced HP values at depth within the East Grampians batholith. From
 403 studies of continental heat flow it has been observed that there is a linear relationship
 404 between the heat production at the surface, A_0 ($\mu\text{W m}^{-3}$), and the surface heat flow, q_0
 405 (mWm^{-2}) (Birch et al, 1968; Roy et al, 1968) i.e.

$$406 \quad q_0 = q^* + A_0 D \quad (5)$$

407 where q^* is the basal or lower crust/mantle heat flow (mWm^{-2}) and D , which has a dimension
 408 of length, represents a depth of radioactive enrichment within the upper crust. Solutions for
 409 calculating the subsurface temperature are given by Wheildon *et al.* (1981) and Wheildon &
 410 Rollin (1986). These take into account the decrease of thermal conductivity with increasing
 411 temperature, which will occur with increasing depth, i.e.

$$412 \quad \lambda_z = \frac{\lambda_0 a'}{(b' + T_z)} \quad (6)$$

413 where λ_z ($\text{W m}^{-1} \text{K}^{-1}$) is the thermal conductivity at depth z (km), λ_0 ($\text{W m}^{-1} \text{K}^{-1}$) is the
 414 surface thermal conductivity, T_z ($^{\circ}\text{C}$) is temperature at depth z , b' is an empirical constant,
 415 with units of $^{\circ}\text{C}$, quoted by Wheildon & Rollin (1986) as 823.33 and $a' = b' + T_0$ (where T_0 is
 416 the surface temperature in $^{\circ}\text{C}$). The vertical temperature distribution is given by Wheildon &
 417 Rollin, (1986) as,

$$418 \quad T_z = a' e^{\frac{(q_0 z - f(z))}{a' \lambda_0}} - b' \quad (7)$$

419 Where for an exponential decrease of heat production with depth, $f(z)$ in equation (7) has the
420 form,

$$421 \quad f(z) = A_0 D \left[z - D \left(1 - e^{-\frac{z}{D}} \right) \right] \quad (8)$$

422 In this case D is the range of depth over which the heat production decreases to $1/e$ (0.37) of
423 its surface value and has been assigned a value of 4 km. Predicted sub-surface temperatures
424 incorporating the revised heat flows are tabulated in Table 2 along with λ_0 and T_0 for each
425 borehole (note that heat production data, A_0 , are given in Table 1). A graphical representation
426 of the sub-surface temperatures is shown in Figure 6. Two predictions are shown for
427 Bennachie, the first (small dashed line) is based on the heat flow of 100.9 mWm^{-2} calculated
428 from the whole depth of the borehole and the second (large dashed line) on the heat flow of
429 89.9 mWm^{-2} calculated from the upper section of the borehole. For the East Grampians
430 batholith as a whole the predicted temperature at 5 km depth is $129 \text{ }^\circ\text{C}$ and at 7 km depth it is
431 $176 \text{ }^\circ\text{C}$, where these mean temperatures have excluded the heat flow calculated from the
432 lower section of the Bennachie borehole where the thermal conductivities appear suspect.
433 The predicted temperatures are dependent on the depth value D . For instance, if $D = 7 \text{ km}$
434 then the equivalent mean temperatures at 5 km and 7 km depth are $126 \text{ }^\circ\text{C}$ and $168 \text{ }^\circ\text{C}$
435 respectively. A value of $D = 4 \text{ km}$ is preferred based on the geological mapping evidence
436 presented above that the HHP character of the granite is likely to be confined to a relatively
437 narrow upper zone of the intrusions.

438 Westaway (2009) and Westaway & Bridgland (2014) also present a solution to the
439 temperature distribution with depth assuming heat production decreases exponentially with
440 depth, but with constant thermal conductivity, i.e.

$$441 \quad T_z = T_0 + \frac{q^* z}{\lambda_0} + \frac{A_0 D^2}{\lambda_0} \left(1 - e^{-\frac{z}{D}} \right) \quad (9)$$

442 With a value of $D = 4 \text{ km}$ and with the same parameters as used above, sub-surface
443 temperature predictions based on equation (9) are also tabulated in Table 2 and shown in
444 Figure 7. The result is a set of slightly reduced geotherms ($-8 \text{ }^\circ\text{C}$ at 5 km and $-15 \text{ }^\circ\text{C}$ at 7 km
445 depth) that illustrates the importance of considering the effect of increasing temperature on
446 thermal conductivity.

447 The revised temperatures of $129 \text{ }^\circ\text{C}$ and $176 \text{ }^\circ\text{C}$ at 5 km and 7 km respectively, compare to
448 temperatures of $92 \text{ }^\circ\text{C}$ at 5 km depth and $118 \text{ }^\circ\text{C}$ at 7 km depth predicted by Wheildon *et al.*
449 1984, corresponding to percentage increases of 40% at 5 km depth and 49% at 7 km depth.

450 These temperatures are lower than expected at similar depths in the Cornubian batholith of
451 Cornwall where temperatures of 182 °C at 5 km depth and 258 °C at 7 km depth were
452 predicted by Downing & Gray (1986a). However, they do indicate a substantially increased
453 resource over that originally predicted for the East Grampians batholith and suggest that
454 power generation could be possible from boreholes drilled to depths greater than 5 km. In
455 addition, the geothermal resource may be accessible as hot water (direct use geothermal).
456 Calcite-cemented breccia, quartz-calcite veins and calcite veins were all described from the
457 cores taken in the heat flow boreholes (Webb & Brown 1984; Webb *et al.* 1985) raising the
458 possibility that there are networks of transmissive fractures at depth from where the calcite
459 has dissolved. Manning *et al.* (2007) measured a fracture permeability of $1.68 \times 10^{-10} \text{ m}^2$
460 within the North Pennine Batholith (Weardale granite) which is the highest measured
461 permeability for a granite within the UK. Although there is no evidence to indicate a fracture
462 permeability of this magnitude within the East Grampians, with predicted temperatures of 58
463 °C at 2 km depth a borehole targeted to intersect a fracture zone could provide a direct use
464 resource for communities within the Cairngorm region.

465 **Conclusions**

466 A rigorous correction for the effects of palaeoclimate on heat flow has been applied to the
467 East Grampians batholith. This has resulted in an increase of 25% over previously reported
468 values to $86 \pm 7 \text{ mWm}^{-2}$. Two scenarios have been followed for the surface temperature
469 history in the Cairngorm region during the last glacial-interglacial
470 cycle due to uncertainty in the extent of ice cover for the period prior to 37 kyr BP. These
471 two scenarios made little difference to the correction demonstrating that in the depth range
472 100-300 m it is warming since the LGM that has been the major influence on perturbing sub-
473 surface temperatures. Recent mapping suggests that the outcropping granites of the East
474 Grampians batholith lie near the surface of a highly evolved magma system. Evidence from
475 other outcropping granites that are probably representative of the Cairngorm, Mount Battock,
476 Ballater and Bennachie intrusions at a few kilometres depth supports the hypothesis that heat
477 production decreases with depth as the rock becomes progressively less siliceous. The
478 coincident, large Bouguer gravity anomaly low has been previously modelled as granite
479 extending to great depth. More recent work on granite emplacement suggests that granite
480 intrusions are more likely to be tabular in form with deep seated, semi-vertical feeder
481 conduits. Such a shape presents more options for creating a model of evolved granite at

482 outcrop with more mafic (and hence denser) rocks at depth. It is recommended that a new 3D
483 gravity model of the East Grampians batholith should be produced.

484 Modelling of sub-surface temperatures that take account of the decrease of heat production
485 and thermal conductivity with depth suggest a temperature of 129 °C at 5 km depth and 176
486 °C at 7 km depth for the East Grampians batholith, increases of 40% and 49% respectively
487 compared to previous estimates. Although these temperatures are currently at the lower end
488 of viability for EGS they indicate that there is a considerable geothermal resource within the
489 batholith. Hydrothermal alteration within the granite indicates the possibility of transmissive
490 fractures at depth that might be exploitable for direct geothermal heat use.

491 **Acknowledgements**

492 This paper is published by permission of the Executive Director of the British Geological
493 Survey (NERC).

494 **References**

- 495 ANNAN J D AND HARGREAVES J C. 2013. A new global reconstruction of temperature changes at the Last
496 Glacial Maximum. *Climate of the Past*, **9**, 367–376.
- 497 BARTLEIN, P, HARRISON, S, BREWER, S, CONNOR, S, DAVIS, B, GAJEWSKI, K, GUIOT, J, HARRISON-PRENTICE, T,
498 HENDERSON, A, PEYRON, O, PRENTICE, I C, SCHOLZE, M, SEPPA, H, SHUMAN, B, SUGITA, S, THOMPSON, R
499 S, VIAU, A E, WILLIAMS, J, AND WU, H. 2011. Pollen-based continental climate reconstructions at 6 and 21
500 ka: a global synthesis, *Climate Dynamics*, **37**, 775–802.
- 501 BATCHELOR, A S. 1987. Development of Hot-Dry-Rock geothermal systems in the UK. *Thermal Power, IEE*
502 *Proceedings*, **134A(5)**, 371–380.
- 503 BEARDSMORE, G R AND CULL, J R. 2001. *Crustal heat flow: a guide to measurement and modelling*. Cambridge:
504 Cambridge University Press.
- 505 BECK, A E. 1977. Climatically perturbed temperature gradients and their effect on regional and continental
506 heat-flow means. *Tectonophysics*, **41**, 17–39.
- 507 BENFIELD, A E. 1939. Terrestrial heat flow in Great Britain. *Proceedings of the Royal Society*, **173A**, 430–450.
- 508 BIRCH, F. 1948. The effects of Pleistocene climatic variations upon geothermal gradients. *American Journal of*
509 *Science*, **246**, 729–760.
- 510 BIRCH, F, ROY, R F AND DECKER, E R. 1968. Heat flow and thermal history in New England and New York.
511 437-451 in *Studies in Appalachian Geology*, AN-ZEN, E (ed), New York: Wiley Interscience.
- 512 BRITISH GEOLOGICAL SURVEY. 1989. *Braemar. Scotland Sheet 65WE. Solid Geology. 1:50 000*. British
513 Geological Survey, Keyworth, Nottingham.
- 514 BRITISH GEOLOGICAL SURVEY. 1992. *Inverurie. Scotland Sheet 76E. Solid Geology. 1:50 000*. British
515 Geological Survey, Keyworth, Nottingham.

- 516 BRITISH GEOLOGICAL SURVEY. 1993a. *Alford. Scotland Sheet 76W. Solid Geology. 1:50 000*. British
517 Geological Survey, Keyworth, Nottingham.
- 518 BRITISH GEOLOGICAL SURVEY. 1993b. *Aviemore. Scotland Sheet 74E. Solid Geology. 1:50 000*. British
519 Geological Survey, Keyworth, Nottingham.
- 520 BRITISH GEOLOGICAL SURVEY. 1995a. *Aboyne. Scotland Sheet 66W. Solid Geology. 1:50 000*. British
521 Geological Survey, Keyworth, Nottingham.
- 522 BRITISH GEOLOGICAL SURVEY. 1995b. *Ballater. Scotland Sheet 65E. Solid Geology. 1:50 000*. British
523 Geological Survey, Keyworth, Nottingham.
- 524 BRITISH GEOLOGICAL SURVEY. 1995c. *Glenbuchat. Scotland Sheet 75E. Solid Geology. 1:50 000*. British
525 Geological Survey, Keyworth, Nottingham.
- 526 BRITISH GEOLOGICAL SURVEY. 1996a. *Banchory. Scotland Sheet 66E. Solid and Drift Geology. 1:50 000*.
527 British Geological Survey, Keyworth, Nottingham.
- 528 BRITISH GEOLOGICAL SURVEY. 1996b. *Glenlivet. Scotland Sheet 75W. Solid Geology. 1:50 000*. British
529 Geological Survey, Keyworth, Nottingham.
- 530 BROWN, G C, WEBB, P C, LEE, M K, WHEILDON, J AND CASSIDY, J. 1982. Development of HDR reconnaissance
531 in the United Kingdom. In: *Proceedings International Conference on Geothermal Energy*, Florence, Italy,
532 BHRA Fluid Engineering, Cranfield, England, 353-367.
- 533 BULLARD, E C. 1939. Heat flow in South Africa. *Proceedings of the Royal Society of London*, **173A**, 428-450.
- 534 BULLARD, E C. 1940. The disturbance of the temperature gradient in the earth's crust by inequalities of height.
535 *Monthly Notices of the Royal Astronomical Society Geophysical Supplement*, **No 4**, 360-362.
- 536 BUSSCHERS, F S, KASSE, C, VAN BALEN, R T, VANDENBERGHE, J, COHEN, K M, WEERTS H J T, WALLINGA, J,
537 JOHNS, C, CLEVERINGA, P AND BUNNICK, F P M. 2007. Late Pleistocene evolution of the Rhine-Meuse
538 system in the southern North Sea basin: Imprints of climate change, sea-level oscillation and glacio-
539 isostasy. *Quaternary Science Reviews*, **26**, 3216–3248.
- 540 CARSLAW, H A AND JAEGER J C. 1959. *Conduction of heat in solids*. 2nd ed. Oxford: Oxford University Press.
- 541 CLAPPERTON, C M. 1997. Greenland ice cores and North Atlantic sediments: implications for the last glaciation
542 in Scotland. In: Gordon, J.E. (Ed.), *Reflections on the Ice Age in Scotland*. Scottish Natural Heritage,
543 Edinburgh, 45–58.
- 544 CLARK, C D, HUGHES, A L C, GREENWOOD, S L, JORDAN, C, SEJRUP, H P. 2012. Pattern and timing of retreat of
545 the last British-Irish Ice Sheet. *Quaternary Science Reviews*, **44**, 112–146.
- 546 CRAIN, I K. 1968. The glacial effect and the significance of continental terrestrial heat flow measurements.
547 *Earth and Planetary Science Letters*, **4**, 69–72.
- 548 CRUDEN, A R. 1998. On the emplacement of tabular granites. *Journal of the Geological Society, London*, **155**,
549 853–862.

- 550 DAVIS, B A S, BREWER, S, STEVENSON, A C, GUIOT, J AND DATA CONTRIBUTORS. 2003. The temperature of
551 Europe during the Holocene reconstructed from pollen data. *Quaternary Science Reviews*, **22**, 1701–1716.
- 552 DOWNING, R. A. AND GRAY, D. A. (eds.) 1986a. Geothermal Energy – The potential in the United Kingdom.
553 HMSO, London.
- 554 DOWNING, R. A. AND GRAY, D. A. 1986b. Geothermal resources of the United Kingdom. *Journal of the*
555 *Geological Society, London*, **143**, 499-507.
- 556 EVANS, D J A, LIVINGSTONE, S J, VIELI, A, O’COFAIGH, C. 2009. The palaeoglaciology of the central sector of
557 the British and Irish Ice Sheet: reconciling glacial geomorphology and preliminary ice sheet modelling.
558 *Quaternary Science Reviews*, **28**,739–757.
- 559 GLASSER, N F AND SIEGERT, M J. 2002. Calculating basal temperatures in ice sheets: an Excel spreadsheet
560 method. *Earth Surface Processes and Landforms*, **27**, 673–680.
- 561 HALL, A M AND GLASSER, N F. 2003. Reconstructing the basal thermal regime of an ice stream in a landscape of
562 selective linear erosion: Glen Avon, Cairngorm Mountains, Scotland. *Boreas*, **32**, 191-207.
- 563 HARRISON, T J. 1987. The evolution of the Eastern Grampian Granites. Unpublished PhD thesis, University of
564 Aberdeen.
- 565 HIGHTON, A J. 1999. Cnoc Mor to Rubh’ Ardlanish. 417–421 in *Geological Conservation Review Series -*
566 *Caledonian Igneous Rocks of Great Britain*. Stephenson D et al. (eds). (Peterborough: Joint Nature
567 Conservation Committee.)
- 568 HUBBARD, A, BRADWELL, T, GOLLEDGE, N, HALL, A, PATTON, H, SUGDEN, D, COOPER, R, AND STOKER, M.
569 2009. Dynamic cycles, ice streams and their impact on the extent, chronology and deglaciation of the
570 British–Irish ice sheet. *Quaternary Science Reviews*, **28**, 758–776.
- 571 JESSOP, A M. 1971. The Distribution of Glacial Perturbation of Heat Flow in Canada. *Canadian Journal of*
572 *Earth Sciences*, **8**, 162–166.
- 573 LEE, M K. 1984. Analysis of geophysical logs from the Shap, Skiddaw, Cairngorm, Ballater, Mount Battock
574 and Bennachie heat flow boreholes. Report in series: *Investigation of the Geothermal Potential of the UK*.
575 British Geological Survey.
- 576 LEE, M K, WHEILDON, J, WEBB, P C, BROWN, G C, ROLLIN, K E, CROOK, C N, SMITH, I F, KING, G and THOMAS-
577 BETTS, A. 1984. Hot dry rock prospects in Caledonian Granites: evaluation of results from the BGS-IC-
578 OU research programme (1981-1984). Report in series: *Investigation of the Geothermal Potential of the*
579 *UK*. British Geological Survey.
- 580 LEE, M K, BROWN, G C, WEBB, P C, WHEILDON, J AND ROLLIN, K E. 1987. Heat flow, heat production and
581 thermo-tectonic setting in mainland UK. *Journal of the Geological Society, London*, **144**, 35–42.
- 582 LEES, C H. 1910. On the shapes of isogeotherms under mountain ranges in radioactive districts. *Proceedings of*
583 *the Royal Society of London*, **83A**, 339–434.

- 584 MANNING, D A C, YOUNGER, P, SMITH, F W, JONES, J M DUFTON, D J AND DISKIN, S. 2007. A deep geothermal
585 exploration well at Eastgate, Weardale, UK: a novel exploration concept for low-enthalpy resources.
586 *Journal of the Geological Society, London*, **164**, 371–382.
- 587 MARGO PROJECT MEMBERS, 2009. Constraints on the magnitude and patterns of ocean cooling at the Last
588 Glacial Maximum. *Nature Geoscience*, **2**, 127–132, doi:10.1038/NGEO411.
- 589 MASLIN, M A, SHACKLETON, N J AND PFLAUMANN U. 1995. Surface water temperature, salinity, and density
590 changes in the northeast Atlantic during the last 45,000 years: Heinrich events, deep water formation, and
591 climatic rebounds. *Paleoceanography*, **10**, 527–544, doi:10.1029/94PA03040.
- 592 MCMANUS, J F, OPPO, D W AND CULLEN, J L. 1999. A 0.5-Million-Year Record of Millennial-Scale Climate
593 Variability in the North Atlantic. *Science*, **283**, 971-975.
- 594 MIT (Massachusetts Institute of Technology). 2006. The Future of Geothermal Energy: Impact of Enhanced
595 Geothermal Systems (EGS) on the United States in the 21st Century. <http://geothermal.inel.gov>.
- 596 NORTH GREENLAND ICE CORE PROJECT MEMBERS, 2004. High-resolution record of Northern Hemisphere
597 climate extending into the last interglacial period. *Nature*, **431**, 147-151.
- 598 PETFORD, N, CRUDEN, A R, MCCAFFREY, K J W AND VIGNERESSE J-L. 2000. Granite magma formation,
599 transport and emplacement in the Earth's crust. *Nature*, **408**, 669-673.
- 600 RICHARDS, H G, PARKER, R H and GREEN, A S P. 1994. The performance and characteristics of the
601 experimental hot dry rock geothermal reservoir at Rosemanowes, Cornwall (1985-1988). *Geothermics*, **23**,
602 73–109.
- 603 ROLLIN, K E. 1982. A review of data relating to hot dry rock and selection of targets for detailed study. Report
604 in series: *Investigation of the Geothermal Potential of the UK*. British Geological Survey.
- 605 ROLLIN, K E. 1984. Gravity modelling of the Eastern Highlands Granites in relation to heat flow studies. Report
606 in series: *Investigation of the Geothermal Potential of the UK*. British Geological Survey.
- 607 ROLLIN, K E. 2009. *Regional Geophysics of Northern Scotland*. Version 1.0 on CD-ROM. British Geological
608 Survey, Keyworth, Nottingham.
- 609 ROY, R F, BLACKWELL, D D AND BIRCH, F. 1968. Heat generation of plutonic rocks and continental heat flow
610 provinces. *Earth and Planetary Science Letters*, **5**, 1-12.
- 611 SHAKUN, J D, CLARK, P U, HE, F, MARCOTT, S A, MIX, A C, LIU, Z, OTTO-BLIESNER, B, SCHMITTNER, A AND
612 BARD, E. 2012. Global warming preceded by increasing carbon dioxide concentrations during the last
613 deglaciation. *Nature*, **484**, 49-54.
- 614 SIEGERT, M J AND DOWDESWELL, J A. 2004. Numerical reconstructions of the Eurasian Ice Sheet and climate
615 during the Late Weichselian. *Quaternary Science Reviews*, **23**, 1273–1283.
- 616 STEPHENS, W E. 1999. Clatteringshaws Dam quarry. 456–459 in *Geological Conservation Review Series -*
617 *Caledonian Igneous Rocks of Great Britain*. Stephenson D et al. (eds). (Peterborough: Joint Nature
618 Conservation Committee.)

- 619 STEPHENS, W E AND HALLIDAY, A N. 1984. Geochemical contrasts between late Caledonian granitoid
620 intrusions of northern, central and southern Scotland. *Transactions of the Royal Society of Edinburgh:*
621 *Earth Sciences*, **75**, 259–273.
- 622 STEPHENSON, D. and GOULD, D. 1995. *British regional geology: the Grampian Highlands* (4th edition).
623 (London: HMSO for the British Geological Survey.)
- 624 STEWART, M A AND LONERGAN, L, 2011. Seven glacial cycles in the middle-late Pleistocene of northwest
625 Europe: Geomorphic evidence from buried tunnel valleys. *Geology*, **39**, 283–286.
- 626 STOKER, M S AND BRADWELL, T. 2005. The Minch palaeo-ice stream, NW sector of the British-Irish Ice Sheet.
627 *Journal of the Geological Society, London*, **162**, 425–428.
- 628 TAYLOR, G K. 2007. Intrusion shapes in the Cornubian Batholith: new perspectives from gravity modelling.
629 *Journal of the Geological Society, London*, **164**, 525-528.
- 630 THOMAS, C W, GILLESPIE, M R, JORDAN , C J and HALL, A M. 2004. Geological structure and landscape of the
631 Cairngorm Mountains. *Scottish Natural Heritage Commissioned Report No. 064* (ROAME No.
632 F00AC103).
- 633 WEBB, P C AND BROWN, G C. 1984. The Eastern Highlands granites: heat production and related geochemistry.
634 Report in series: *Investigation of the Geothermal Potential of the UK*. British Geological Survey.
- 635 WEBB, P C, TINDLE, A G, BARRITT, S D, BROWN, G C AND MILLER, J F. 1985. Radiothermal granites of the
636 United Kingdom: comparison of fractionation patterns and variation of heat production for selected
637 granites. 409–424 in *High heat production (HHP) granites, hydrothermal circulation and ore genesis*.
638 (The Institution of Mining and Metallurgy.)
- 639 WESTAWAY, R. 2009. Quaternary uplift of northern England. *Global and Planetary Change*, **68**, 357-382.
- 640 WESTAWAY, R AND BRIDGLAND D R. 2014. Relation between alternations of uplift and subsidence revealed by
641 Late Cenozoic fluvial sequences and physical properties of the continental crust. *Boreas*, **43**, 505-527.
- 642 WESTAWAY, R AND YOUNGER, P L. 2013. Accounting for palaeoclimate and topography: A rigorous approach to
643 correction of the British geothermal dataset. *Geothermics*, **48**, 31-51.
- 644 WHEILDON, J, KING, G, CROOK, C N AND THOMAS-BETTS, A. 1984. The Eastern Highlands granites: heat flow,
645 heat production and model studies. Report in series: *Investigation of the Geothermal Potential of the UK*.
646 British Geological Survey.
- 647 WHEILDON, J, FRANCIS, M F, ELLIS, J R L AND THOMAS-BETTS, A. 1981. Investigation of the south-west
648 England thermal anomaly zone. Report EUR 7276EN. (Brussels: CEC).
- 649 WHEILDON, J AND ROLLIN, K E. 1986. Heat Flow. 8-20 in *Geothermal Energy – The potential in the United*
650 *Kingdom*, DOWNING, R. A. AND GRAY, D. A. (eds.) 1986. HMSO, London.
- 651 YOUNGER, P L, GLUYAS, J G AND STEPHENS, W E. 2012. Development of deep geothermal energy resources in
652 the UK. *Institute of Civil Engineers Proceedings*, **165** (EN1), 19–32.
- 653

Figure 1. Distribution of granite within the crust of Scotland based on surface exposure and interpretations of gravity data. Heat production (in units of μWm^{-3}) are shown for intrusions where values greater than $3.5 \mu\text{Wm}^{-3}$ have been measured.

Figure 2. Shaded relief image, illuminated from the north, of the Bouguer gravity anomaly over the East Grampians batholith, based on gravity data from the British Geological Survey national gravity databank. The outlines of outcropping granites are shown in red and the locations of the four heat flow boreholes are indicated by white crosses.

Figure 3. Selected temperature proxy records used to construct the average temperature trends over the UK during the past 140 kyr. References from top to bottom: A) Davis et al. (2003); B) Shakun et al. (2012); C) Maslin et al. (1995); D) McManus et al. (1999). SST is sea surface temperature and G-IG range is glacial-interglacial range.

Figure 4. The reconstructed UK temperature trend for the last 120 kyr (B) scaled to the temperature at the Cairngorm latitude, aside the appended data used from several sources and regions to create the record (A; see also Figure 3). Ice core temperature proxy shown for comparison (C; North Greenland Ice Core Project members, 2004).

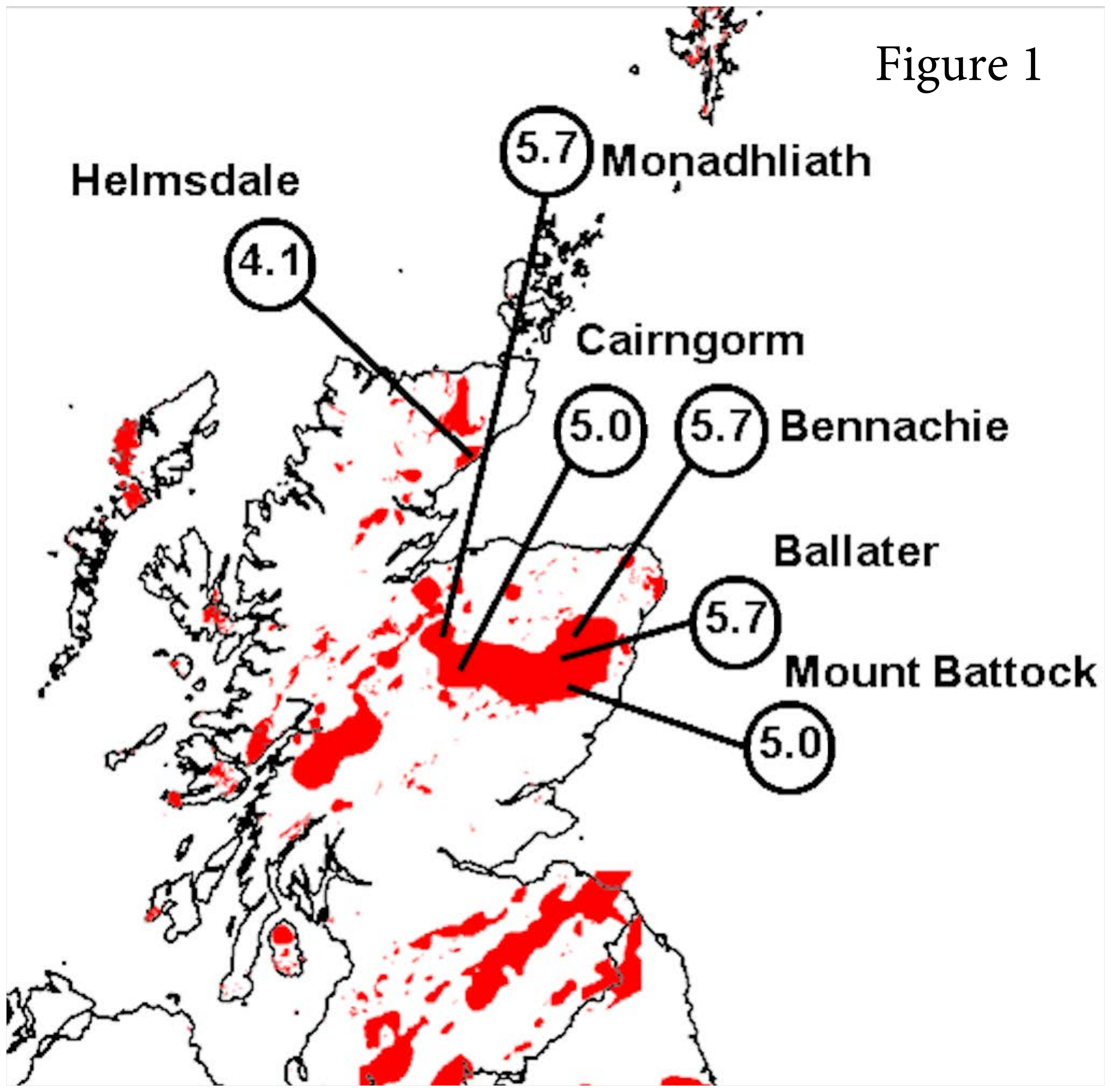
Figure 5. a) Surface temperature history for scenario 1 where continuous ice cover has been assumed for the period 110-12 kyr BP. The solid line is for Cairngorm and where this differs for Mount Battock, Bennachie and Ballater it is shown by the dashed line. b) Surface temperature history for scenario 2 where ice cover has been assumed for the period 37-12 kyr BP only. The solid line is for Cairngorm and where this differs for Mount Battock, Bennachie and Ballater it is shown by the dashed line.

Figure 6. Predicted sub-surface temperatures, based on the revised heat flow estimates, assuming heat production decreases exponentially with depth. A) Thermal conductivity decreases with temperature and B) thermal conductivity is assumed to be constant. In (A), the revised mean temperatures of 129°C at 5 km depth and 176°C at 7 km depth are displayed as stars. Note that two predictions are shown for Bennachie, where the solid line uses heat flow calculated from the whole borehole and the dashed line from the upper section only.

Table 1. Tabulated values of heat production, uncorrected heat flow and corrections to heat flow with a final value of corrected heat flow for the East Grampians heat flow boreholes. The palaeoclimate correction scenarios and the two Bennachie borehole options are explained in the text. Note that the heat production data are from Webb & Brown (1984) and the topographic correction is taken from Wheildon *et al.* (1984).

Table 2. Predicted temperatures at depth arising from the revised heat flow estimates. Heat production is assumed to decrease with depth exponentially for two cases. In the first, the temperature dependence of thermal conductivity is taken into account and in the second, it is assumed to be constant.

Figure 1



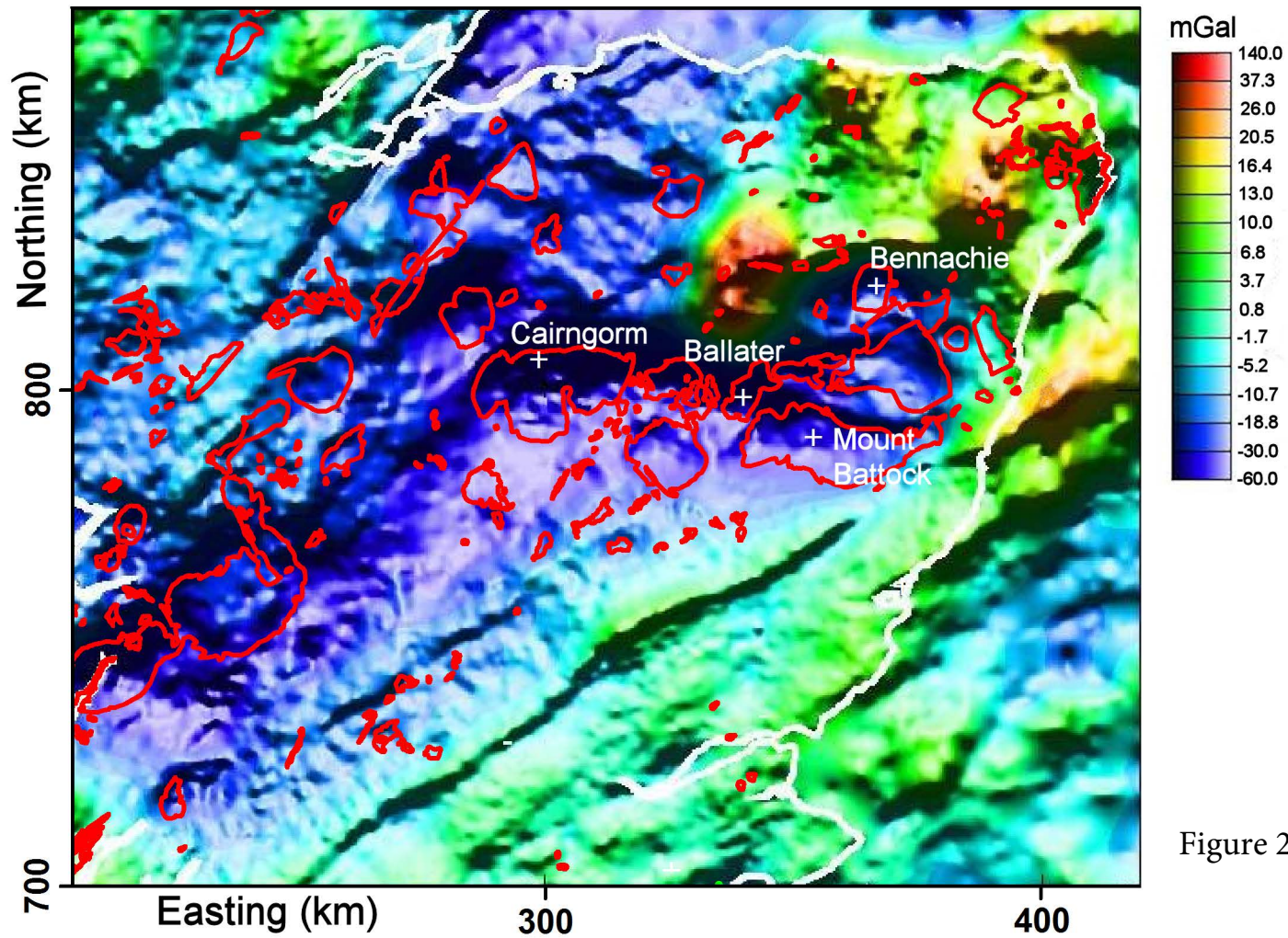


Figure 2

Figure 3

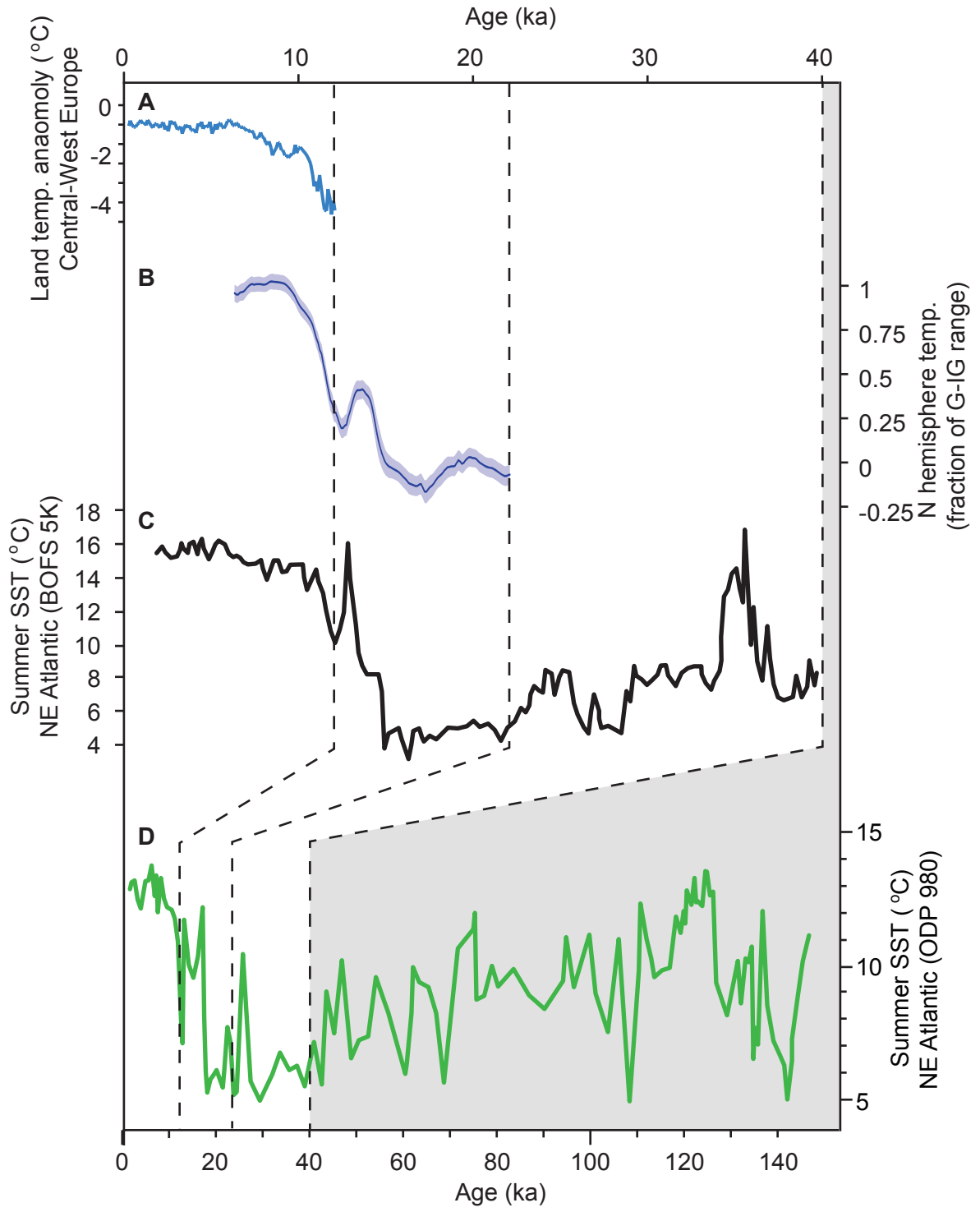


Figure 4

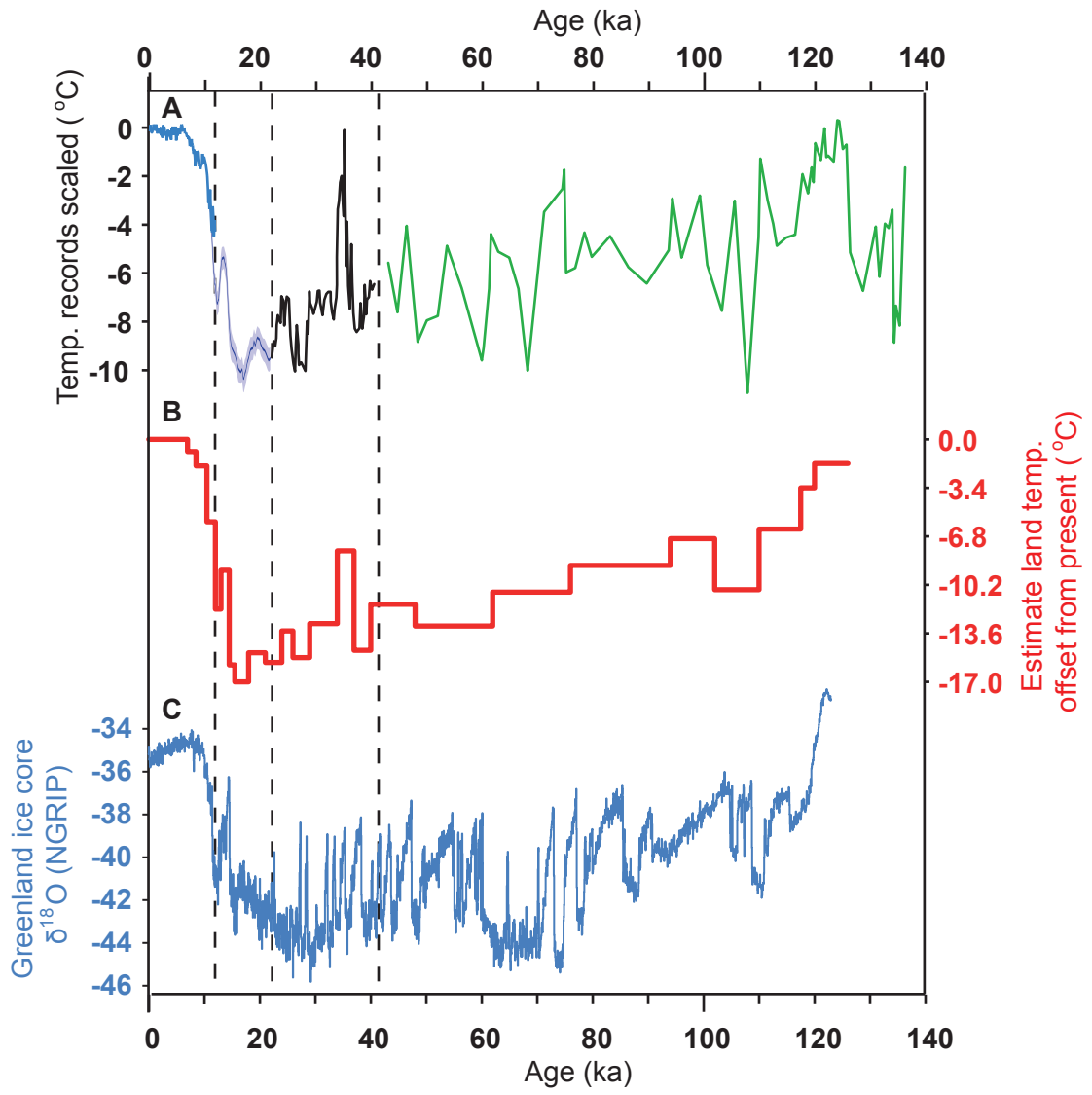


Figure 5a

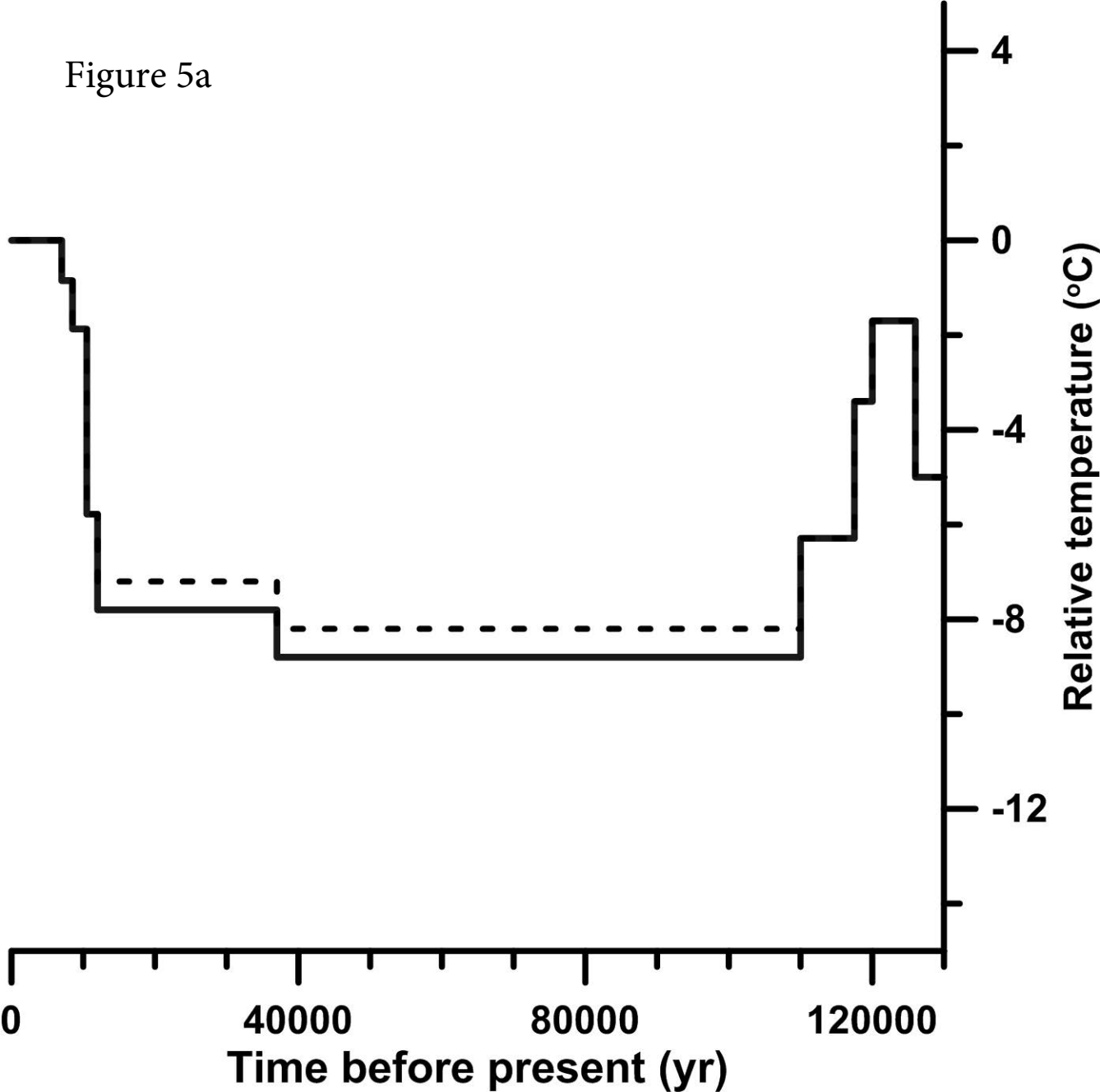
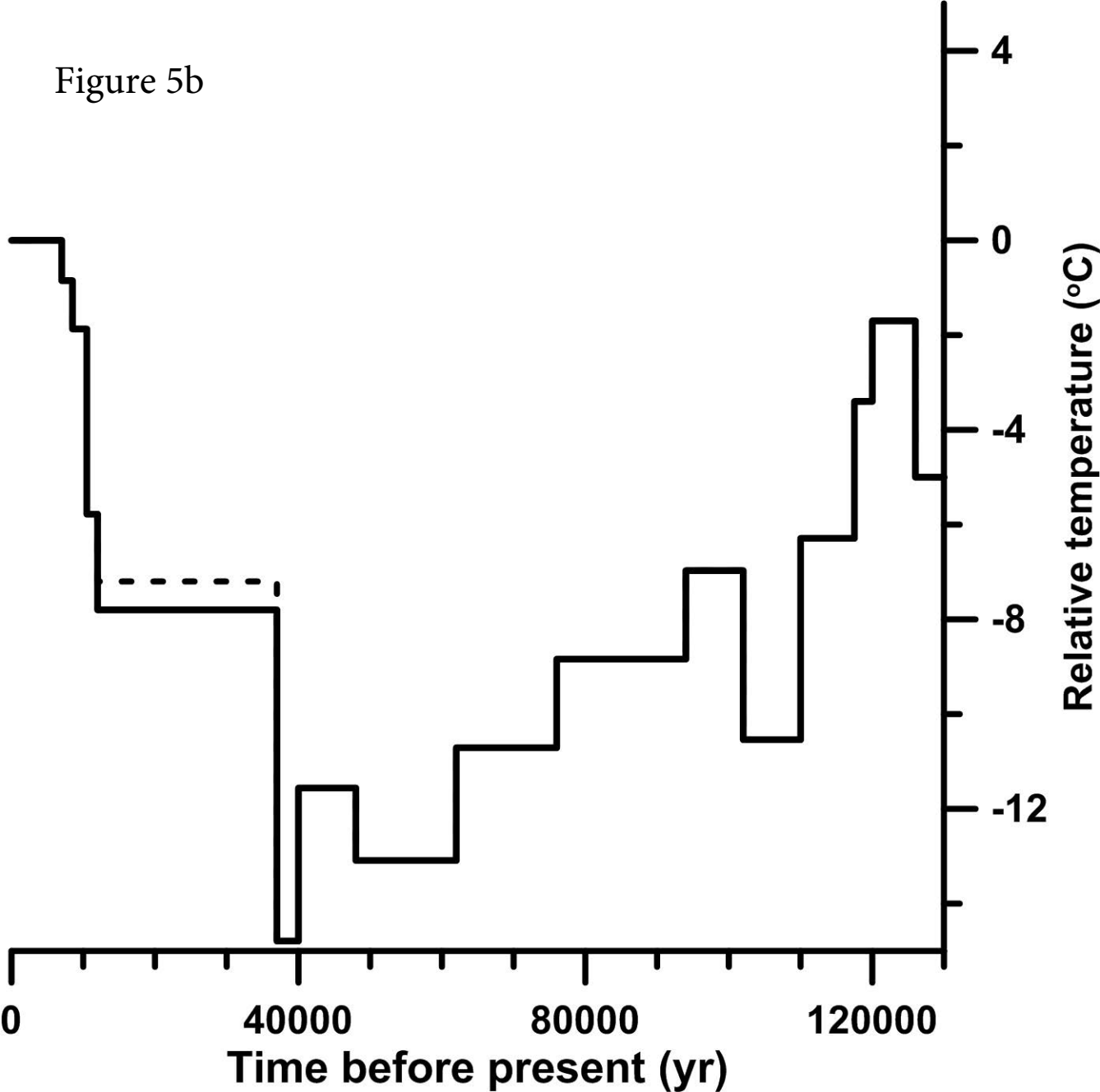


Figure 5b



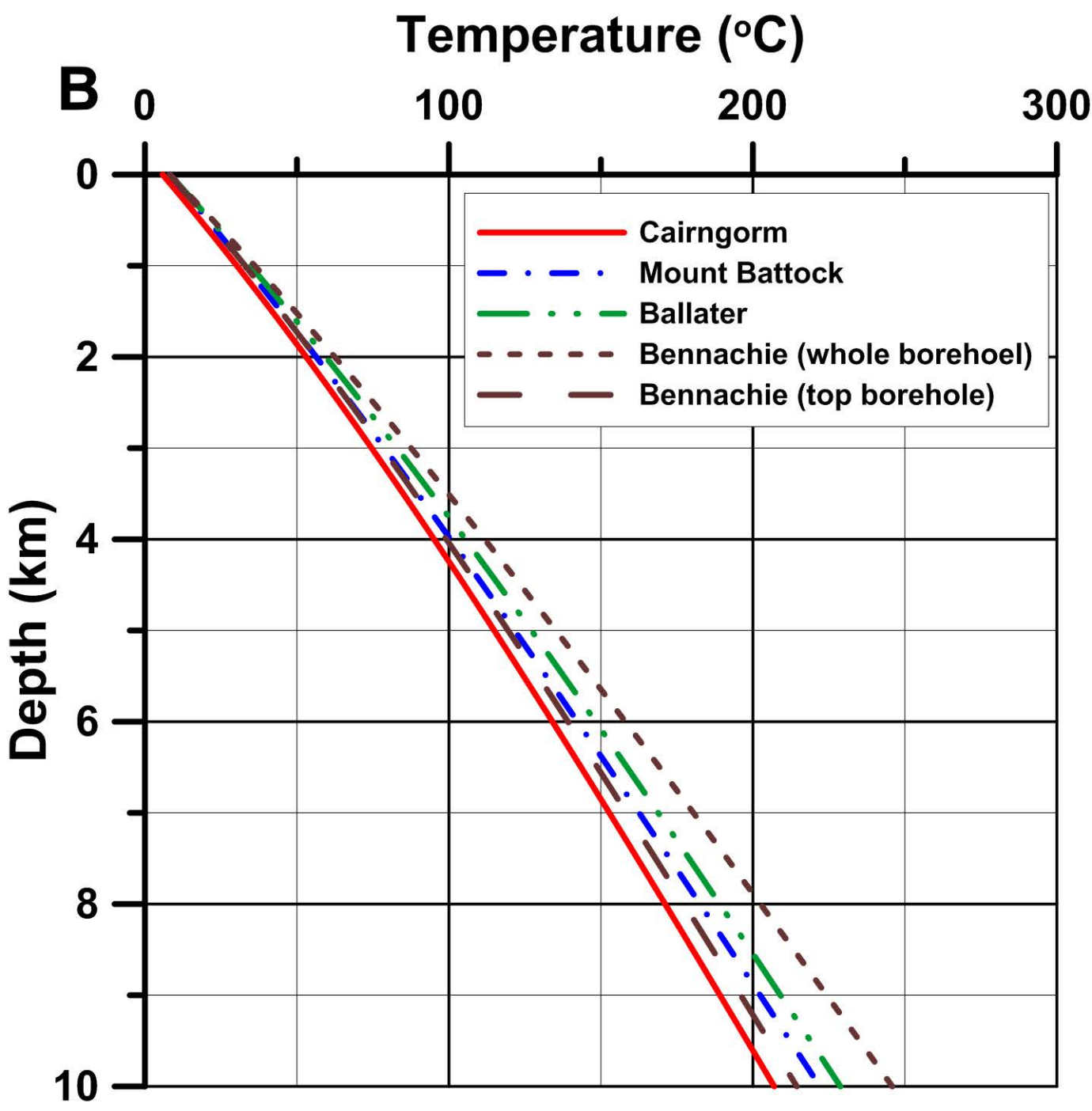
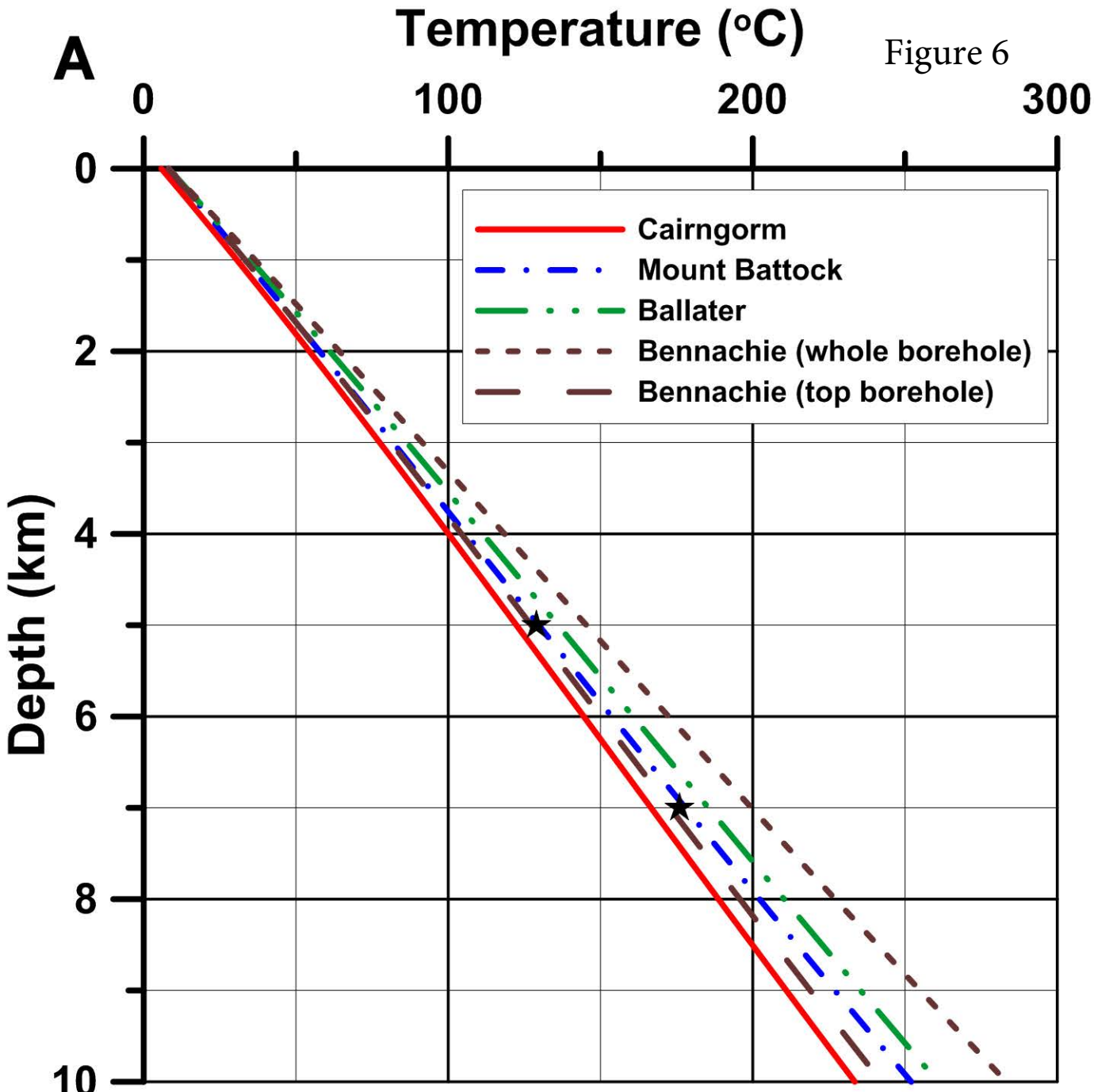


Table 1

Borehole	Heat production, A_0 ($\mu\text{W m}^{-3}$)	Uncorrected heat flow (mW m^{-2})	Palaeoclimate correction (mW m^{-2})			Topographic correction (mW m^{-2})	Corrected heat flow, q_0 (mW m^{-2})
			Scenario 1	Scenario 2	Mean		
Cairngorm	7.3	71.3 ± 2.8	19.6 ± 0.5	21.0 ± 0.4	20.3 ± 0.5	-2.7	88.9 ± 2.8
Mount Battock	4.8	65.0 ± 2.2	17.4 ± 0.4	19.1 ± 0.4	18.2 ± 0.4	-6.9	76.3 ± 2.2
Ballater	6.8	74.1 ± 3.4	16.8 ± 1.3	19.0 ± 0.8	17.9 ± 1.1	-4.2	87.8 ± 3.6
Bennachie (whole borehole)	7.0	85.8 ± 13.2	19.6 ± 1.8	21.7 ± 1.7	20.7 ± 1.7	-5.6	100.9 ± 13.3
Bennachie (top borehole)	7.0	76.1 ± 2.1	18.3 ± 0.4	20.4 ± 0.4	19.4 ± 0.4	-5.6	89.9 ± 2.1

Table 2

Borehole	Surface temperature, T_0 ($^{\circ}\text{C}$)	Surface thermal conductivity, λ_0 ($\text{W m}^{-1} \text{K}^{-1}$)	Predicted temperature at 5 km depth ($^{\circ}\text{C}$)		Predicted temperature at 7 km depth ($^{\circ}\text{C}$)	
			Temperature dependent thermal conductivity	Constant thermal conductivity	Temperature dependent thermal conductivity	Constant thermal conductivity
Cairngorm	5.8	3.5	122	115	167	153
Mount Battock	8.2	3.0	130	122	178	163
Ballater	8.2	3.2	136	127	185	169
Bennachie (whole borehole)	8.2	3.5	145	135	200	180
Bennachie (top borehole)	8.2	3.5	127	119	173	158
Mean (excluding Bennachie whole borehole)			129	121	176	161